The Journal of Chemical Physics

Intrinsic viscosity of small spherical polyelectrolytes: Proof for the intermolecular origin of the polyelectrolyte effect

Markus Antonietti, Andreas Briel, and Stephan Förster

Citation: J. Chem. Phys. **105**, 7795 (1996); doi: 10.1063/1.472605
View online: http://dx.doi.org/10.1063/1.472605
View Table of Contents: http://jcp.aip.org/resource/1/JCPSA6/v105/i17
Published by the AIP Publishing LLC.

Additional information on J. Chem. Phys.

Journal Homepage: http://jcp.aip.org/
Journal Information: http://jcp.aip.org/about/about_the_journal
Top downloads: http://jcp.aip.org/features/most_downloaded
Information for Authors: http://jcp.aip.org/authors

ADVERTISEMENT

Downloaded 28 Aug 2013 to 129.15.14.53. This article is copyrighted as indicated in the abstract. Reuse of AIP content is subject to the terms at: http://jcp.aip.org/about/rights_and_permissions

Intrinsic viscosity of small spherical polyelectrolytes: Proof for the intermolecular origin of the polyelectrolyte effect

Markus Antonietti,[a] Andreas Briel, and Stephan Förster
Max Planck Institut für Kolloid- & Grenzflächenforschung, Kantstrasse 55, D-14513 Teltow-Seehof, Germany

(Received 15 March 1996; accepted 18 July 1996)

Spherical polystyrenesulfonate particles in the size range between 7 nm$<R<$50 nm are synthesized via crosslinking copolymerization in microemulsion and subsequent sulfonation via polymer reactions. These model polyelectrolytes, when carefully purified, show the qualitative aspects of the polyelectrolyte effect, i.e., large excess viscosities with a strong increase of the intrinsic viscosity with decreasing concentration. A quantitative evaluation of these data on the basis of a modified Hess–Klein relation reveals that the complete dependence on polymer as well as on salt concentration can be fitted with one parameter only, the effective charge number per particle, Z_{eff}. The specific viscosity increases with decreasing particle size and inverse particle density, but no simple explanations for the found relations can be given. Since conformational changes play only a minor role for spherical systems, the comparison of the concentration dependence of the reduced viscosities of linear chains with those of the spherical polyelectrolytes allows for a differentiation between intra- and intermolecular effects. It is qualitatively shown that a major contribution to the polyelectrolyte effect is caused by intermolecular interactions, i.e., the increase of the electrostatic screening length and interparticle-coupling with decreasing concentration. The quantitative description of the concentration and molecular weight dependence of the reduced viscosity of linear polyelectrolytes in salt-free solution reveals that Z_{eff} does apparently not depend on molecular weight, the found molecular weight dependence of the reduced viscosity is due to the increase of the hydrodynamic radius, only. In addition, our modified Hess–Klein model also describes some quantitative features of the viscosity curves, such as the molecular weight dependent shape of the maxima. Deviations between theoretical description and experimental data which become significant for smaller linear polyelectrolytes are attributed to a concentration dependent coil expansion. © *1996 American Institute of Physics.* [S0021-9606(96)51840-4]

I. INTRODUCTION

Polyelectrolytes, although among the ''primary rocks'' of polymer science and application, still belong to the poorly understood polymer systems. Recently, two excellent reviews appeared which underline this thesis and point out the necessities for a better and quantitative understanding for the underlying phenomena.[1,2] Even the most familiar phenomenon which is also the base of most polyelectrolyte applications, the sharp increase of the reduced specific viscosity with decreasing concentration (the polyelectrolyte effect), is still discussed in many textbooks of polymer science as a reflection of the rod-coil-transition, i.e., as an intramolecular phenomenon.[3,4] On the other hand, modern theories of polyelectrolyte hydrodynamics describe this effect as purely electrostatic in nature, i.e., caused by intermolecular forces,[5–7] although intramolecular cannot be excluded.

An additional motivation for the present examination arised from very precise static and dynamic light scattering examinations on highly diluted polyelectrolyte solutions;[8] here it was shown that the concentration dependence of the electrostatic persistence length essentially goes with the Debye length, and that the classical Skolnik–Odijk–Fixman theory clearly overestimates the electrostatic stiffening as well as its concentration dependence.[9,10] Schmidt *et al.* pointed out that this difference is due to the neglection of entropic effects of the chain conformation.[11] In any case, the remainder of the stiffening is not big enough to explain the observed viscosity effects.

The approach of the present paper to this problem is somewhat different and motivated by synthetic progress of polymer chemistry; spherical polyelectrolyte molecules with molecular weights comparable to linear polyelectrolytes should be ideal model systems for testing all theories, since they are not expected to perform a rod-coil transition. This idea was already presented by Ise *et al.* in a series of papers[12–14] dealing with the solution viscosity of carefully deionized latex suspensions. Restricted by the limited availability of smaller latex spheres, these experiments were performed at rather low particle number densities and consequently describing only weak effects.

A recently developed synthetic technique, the polymerization in microemulsions, gives access to a new type of model polymers with spherical shape and comparatively small molecular weights, the microgels. These polymer molecules are narrowly distributed and have sizes in the range of 5 nm$<R<$50 nm.[15–17] It is now straightforward to transfer these microgels into polyelectrolyte structures using polymer-analogous reactions which preserve the molecular

[a]Author to whom correspondence should be addressed.

Downloaded 28 Aug 2013 to 129.15.14.53. This article is copyrighted as indicated in the abstract. Reuse of AIP content is subject to the terms at: http://jcp.aip.org/about/rights_and_permissions

shape; the resulting polyelectrolyte microgels can be understood as highly charged, swollen network ''sponges'' with well defined geometry, size, and polydispersity.

The solution viscosity of these polyelectrolyte microgels is examined in dependence of particle size, cross-linking density as well as in dependence of polymer and salt concentrations. The resulting data are described by different theoretical approaches for the solution viscosity of polyelectrolytes.

The behavior of charged microgels is also compared with the corresponding data of linear polyelectrolytes, and some ways to relate the viscosity behavior for the different particle sizes and topologies are proposed. At the end, an estimate of the role of intra- and intermolecular contributions for linear polyelectrolytes is given.

II. THEORY

A. The viscosity

The shear viscosity η can formally be derived from the various forces F acting on a volume element in the solution

$$F=\sum_i \nabla\sigma_i=\eta\nabla^2\mathbf{v}. \tag{1}$$

The local forces derive from local stresses σ that lead to local velocity gradients $\nabla\mathbf{v}$. In case of polyelectrolyte solutions the stresses σ are due to mainly hydrodynamic and electrostatic interactions. To a good approximation, the electrostatic interaction of weakly charged particles can be viewed as a perturbation to otherwise purely hydrodynamic interactions. In the other extreme of highly charged particles, the hydrodynamics may be viewed as a perturbation to an electrostatically coupled system. Starting points theoretically are on the one hand Einstein's treatment of dilute suspensions of noninteracting spheres (I), on the other hand the theory developed by Hess and Klein for highly charged particles (II). The perturbation correction to the Einstein-case (III) consists of introducing an increased effective radius of the particle due to the presence of an ionic atmosphere. A way to treat the perturbation to the Hess–Klein case (IV) is less clear. In the following we briefly outline the available theoretical descriptions.

(I) Einstein derived for the specific viscosity η_{sp} of dilute suspensions of noninteracting spheres

$$\eta_{\mathrm{sp}}=\frac{\eta-\eta_0}{\eta_0}=2.5\phi, \tag{2}$$

where η_0 is the viscosity of the solvent and ϕ the volume fraction of spheres. Following Einstein, the reduced viscosity $\eta_{\mathrm{red}}=\eta_{\mathrm{sp}}/c_p$ can be transferred into molecular parameters,

$$\lim_{c,\dot{\gamma}\to 0}\eta_{\mathrm{red}}\equiv[\eta]=\frac{10}{3}\pi N_A\frac{R_\eta^3}{M}. \tag{3}$$

Here, M_w is the molecular weight of the colloids, and R_η the viscometric radius. For nondrained spheres, geometric radius and viscometric radius are practically identical. c_p denotes the polymer concentration in g/ℓ; molar concentrations throughout the paper are denoted with c'.

For higher concentrations, it is necessary to include the influence of binary hydrodynamic interactions to the viscosity. This is classically done in the Huggins expansion,

$$\eta_{\mathrm{red}}(c_p)=[\eta]+k_H\cdot[\eta]^2\cdot c_p. \tag{4}$$

Here, k_H is the Huggins constant which depends on molecular architecture and interactions; for noninteracting spheres, $k_H=0.64$.

(II) For a derivation the viscosity of charged Brownian particles, one has to return to the description by statistical thermodynamics. The starting point is the Green–Kubo relation for the viscosity of simple liquids,

$$\eta=\frac{1}{kTV}\lim_{q\to 0}\int_0^\infty dt\langle\sigma_{xz}(\mathbf{q},t)\sigma_{xz}(-\mathbf{q},0), \tag{5}$$

which relates the viscosity to fluctuations in the microscopic stresses. Here, σ_{xz} $(\mathbf{q},t)$ is a nondiagonal element of the qth Fourier component of the microscopic stress tensor, related to the transversal component of the microscopic mass current by $(d/dt)j_x(\mathbf{q},t)=iq\sigma_{xz}(\mathbf{q},t)$. As stated above, the Green–Kubo relations applies only to simple liquids. The corresponding Green–Kubo-type equation for Brownian systems involves reduced time evolution and projection operators and is discussed in detail by Hess and Klein in Ref. 5. From this equation Hess and Klein derived a simple equation for the reduced viscosity of charged Brownian particles within the framework of the mode-coupling approximation (MCA). Using the short-time approximation of the dynamic structure factor, i.e., $S(q,t)=S(q)\exp[-q^2Dt/S(q)]$, they derived for the specific viscosity

$$\eta_{\mathrm{sp}}=\frac{\zeta c^2}{60(2\pi)^3}\int d^3q\left[\frac{d}{dq}h(q)\right]^2, \tag{6}$$

where $h(q)$ is the Fourier transform of the total correlation function which is related to the structure factor by $S(q)=1+ch(q)$. Approximations for $h(q)$ can be obtained from integral equation schemes (MSA, HNC, etc.). Within the weak coupling approximation (WCA) the total correlation function can be approximated by $h(q)=-U(q)/kT$. The WCA should apply to weakly charged spherical particles at concentrations small enough that hard-core interactions are of no importance. For charged colloids in the WCA, one can approximate the possibly rather complex potentials with the repulsive part of the DLVO-potential,

$$U(q)=\frac{Z_{\mathrm{eff}}^2e^2}{\epsilon\epsilon_0}\frac{1}{\kappa^2+q^2}\frac{\exp[2\kappa R]}{(1+\kappa R)^2}, \tag{7}$$

where ϵ is the dielectric constant, R is the particle radius, Z_{eff} is the effective charge number per polymer which is discussed in more detail below, and κ is the Debye–Hückel constant given by

$$\kappa^2=4\pi l_B N_L\sum_i Z_i^2c_i', \tag{8}$$

Downloaded 28 Aug 2013 to 129.15.14.53. This article is copyrighted as indicated in the abstract. Reuse of AIP content is subject to the terms at: http://jcp.aip.org/about/rights_and_permissions

$$l_B = \frac{e^2}{4\pi\epsilon\epsilon_0 kT}. \tag{9}$$

The length where electrostatic energy and thermal energy balance is called the Bjerrum length l_B, c_i' and Z_i are the molar concentrations and effective charge numbers of all ionic species i, respectively.

Inserting $U(q)$ in the expression for η and replacing the diffusion coefficient by the corresponding hydrodynamic radius r_H, one obtains

$$\frac{\eta - \eta_0}{\eta_0} = \tfrac{1}{160}\,(4\pi l_B N_L)^2 r_H \frac{Z_{\text{eff}}^4 c'^2}{\kappa^3} \frac{\exp[2\kappa R]}{(1+\kappa R)^2}, \tag{10}$$

which for $\kappa R \ll 1$ reduces to the well-known result first given by Hess and Klein

$$\eta_{\text{red}} = \frac{1}{160}\left(\frac{4\pi l_B N_L}{M_w}\right)^{1/2} r_H \frac{Z_{\text{eff}}^4 c_p}{\left(\frac{2M_s^2}{Mp}\, c_s' + Z c_p\right)^{3/2}}. \tag{11}$$

Here, we employ a version which was rewritten in terms of the specific notations of polymer analysis.[18] M_p is the molecular weight of the polymer and M_s the molecular weight of the salt. It must be noted that the Hess–Klein equation reduces to the empirical Fuoss–Strauss relation $\eta_{\text{red}} \sim c_p^{-1/2}$ (Refs. 19, 20, 21) in the limit $c_p \gg c_s$.

(III) As a perturbation correction to the Einstein case, an effective radius may be introduced. In the perturbation theory by Barker and Hendersen the effective hard sphere diameter is chosen such that

$$R_{\text{el}} = R_0 + \int_{R_0}^{r'} \left[1 - \exp\left(-\frac{\phi}{kT}\right)\right] dr, \tag{12}$$

where r' is the distance where the electrostatic potential ϕ has decayed to zero. Inserting the potential $U(q)$ from Eq. (7), Russel *et al.*[22] obtained for R_{el},

$$R_{\text{el}} = R_0 + \frac{1}{2\kappa} \ln(\alpha/\ln\{\alpha/\ln[\alpha/\ln(\alpha/\ldots)]\}) \tag{13}$$

with

$$\alpha = Z_{\text{eff}}^2 \cdot l_B \kappa \frac{\exp[2\kappa R]}{(1+\kappa R)^2}. \tag{14}$$

At high ionic strength where electrostatic interactions are effectively screened, $R_{\text{el}} \to R_0$.

A question is how to handle such a perturbation correction in the limit of low ionic strength where electrostatic interactions dominate. A possible consistent description, which is motivated by our experimental results, is to postulate that at low ionic strength a maximum radius R_{tot} is reached concomitant with an electrostatic coupling to other particles (Hess–Klein case). R_{tot} may be introduced in an analogous fashion to Eq. (12),

$$R_{\text{tot}} = R_0 + \tfrac{1}{2}\, Z_{\text{eff}}^2 \cdot l_B. \tag{15}$$

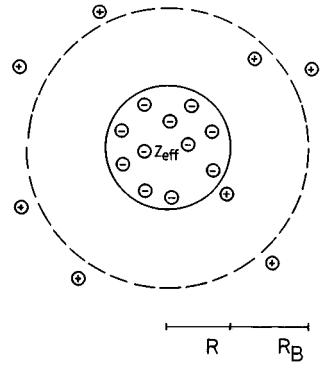

FIG. 1. Concept of the ''Bjerrum shell.'' Each charged colloidal particle with radius R is surrounded of a shell where the electrostatic energy exceeds the thermal energy kT. Counterions inside this shell are regarded to be coupled. The Bjerrum shell with thickness r_B is not accessible for other, similarly charged particles.

This may be viewed as the build-up of a ''Bjerrum shell'' of thickness $R_B = Z_{\text{eff}}^2 \cdot l_B/2$ much like the build-up of a double layer or Stern layer. Overall, with decreasing ionic strength the effective radius of a particle increases from $R_0 \to R_{\text{el}} \to R_{\text{tot}}$ which seems to be supported by our experimental results (see below). Alternatively, R_B may be introduced for all ionic strength, thereby defining an effective ionic strength dependent charge Z_{eff}. At high ionic strength where electrostatic interactions are effectively screened, $Z_{\text{eff}} \to 0$.

The concept of a ''Bjerrum-shell'' around a charged polyelectrolyte-sphere is visualized in Fig. 1.

(IV) The Debye–Hückel law is an exact limiting law in the limit $\kappa R < 1$, where the size of the particles is negligibly small (point charges). Therefore for small particles in the weak coupling approximation the viscosity will follow a $c^{-(1/2)}$ law. For larger particles, size effects and hydrodynamic interactions become appreciable, and expressions for $h(q)$ have to be derived from more complicated equations like the mean-spherical approximation, which is out of the scope of the present paper. As an effect, $h(q)$ becomes a weaker function of κ leading to higher exponents in the concentration dependence. As an illustration, the function $h(q) = (1/kT)(1/\kappa^b + q^2)$ ($b=2$ in the Debye–Hückel limit) leads to $(\eta/c) \sim c\kappa^{-(3b/2)} \sim c^{-(4-3b/4)}$. If $b = 5/3$, one would observe a $c^{-1/4}$-law. Still weaker dependencies would lead to even higher exponents which would eventually become positive. Not affected by assumption of a certain potential, it must be underlined that the minimal scaling exponent which has to be expected is the one of the potential with the widest range, i.e., the Debye–Hückel potential and the $c^{-(1/2)}$-law.

The meaning of Z_{eff} will play an important role in the following discussions. Z_{eff} is the effective charge number per particle which is obtained by rescaling the complicated multi ion–ion interactions to a screened Coulomb potential. Since there is—to our knowledge—no simple way to calculate Z_{eff} for a charged extended object in presence of low molecular weight ions, Z_{eff} is treated as a significant fit parameter without any clear physical meaning.

Downloaded 28 Aug 2013 to 129.15.14.53. This article is copyrighted as indicated in the abstract. Reuse of AIP content is subject to the terms at: http://jcp.aip.org/about/rights_and_permissions

To describe experimental results, the contributions from stresses arriving from hydrodynamics (III) and electrostatics (II) may simply be summed up as suggested by Eq. (1). This is a very crude approximation (which neglects possible cross-terms), but—to our knowledge—the best we can do. As a result that can be tested experimentally we arrive at the expression

$$\eta_{\mathrm{red}}=[\eta]_0+k_H[\eta]_0^2\cdot c_p+\frac{1}{160}\cdot r_H\cdot\left(\frac{4\pi e^2\cdot N_L}{M_P\cdot\epsilon\epsilon_0 kT}\right)^{1/2}\cdot\frac{Z_{\mathrm{eff}}^4 c_p}{\left(2\cdot\frac{M_P}{M_S}c_s+Z_{\mathrm{eff}}c_p\right)^{3/2}} \tag{16}$$

with

$$[\eta]_0=\frac{10}{3}\pi N_A\cdot\frac{1}{M_P}\cdot(R_0+R_B)^3$$

and

$$r_H=R_0. \tag{17}$$

Equation (17) splits the size of the polyelectrolyte spheres in a geometric radius R and the additional Bjerrum radius R_B, an ansatz which was discussed above. Since R_B is also related Z_{eff} this equation posesses only two fitting parameters, R_B and k_H, where k_H can be fixed to be in the order of the ideal value of a sphere.

III. EXPERIMENT

A. Polymer synthesis

The technique of polymerization in microemulsions has recently be reviewed[17] and should for the present context just briefly be recapitulated. For the smaller particles in the range of $5<R<12$ nm, the metallosurfactant myristyldiethanolamin-copper was used[16] whereas for all other systems cetyltrimethylammoniumchloride (CTMA) was taken as the surfactant.[15]

Typically, 10 g of freshly distilled styrene, the designated amount of crosslinker (e.g., 0.38 g *m*-diisopropenylbenzene for a crosslinking density of 1/10 or one crosslink per 10 monomer units), and 150 mg of AIBN were mixed to form the oil phase. A solution of the calculated amount of surfactant [e.g., 20 g CTMA (Aldrich) or myristyldiethanolamine-copper, synthesized according to Ref. 16] in deionized and degassed water was prepared separately (100 g altogether). Oil and water phase were mixed. Microemulsification occurs spontaneously in case of the metallosurfactant whereas for the CTMA system, vigorous stirring with a high speed stirrer is helpful. After approach of equilibrium, the reaction mixtures were heated for 24 h at 60–70 °C. After this reaction time, the conversions exceeded 90%, as checked by the mass of the isolated polymer.

An aliquot of the latex was kept for characterization with dynamic light scattering and electron microscopy, the remainder was precipitated by addition of 200 mℓ of methanol. The surfactants were removed by a threefold reprecipitation. Here, the crude product was redissolved in 100 mℓ THF and precipitated in methanol by dropwise addition of the microgel solutions. The resulting white powder was dried in the vacuum oven for 48 h at 50 °C.

Sulfonation of these microgels was performed either with H_2SO_4/P_2O_5 according to the Vink-procedure[23] or with a newly developed synthesis using H_2SO_4/Ac_2O in 1,2-dichloroethane.[24] Model reactions with narrowly distributed polystyrene standards which are characterized after sulfonation by aqueous GPC showed only a very weak influence of chain scission or crosslinking reactions.[24] These linear model polyelectrolytes were also used for viscosity measurements. The PSS was dialyzed and used as a 1% solution in water.

Polystyrene latex particles with high surface density of sulfonate groups, small particle size, and narrow particle size distribution were made by emulsion polymerization using surfmers and subsequent fractionation with the preparative ultracentrifuge. The synthesis of these particles is described in more detail in a different context.[25]

B. Particle size characterization

The particle sizes and particle size distributions were determined by thermal field flow fractionation (TFFF) coupled with multiangle laser light scattering (MALLS) detection. The TFFF system used in this work was constructed and assembled in a similar way as those used in previously reported thermal FFF studies.[26] All further details of the setup as well as its separation properties for complex and functionalized systems was published in a separate paper.[27]

Dynamic light scattering for the characterization of the parental polystyrene microgels was carried out using a Nicomp C370 particle sizer with the ability of multiangle detection. Only correlations with excellent contrast and correlation strengths above 0.6 were taken. Using the software of the particle sizer, the correlation functions were fitted with a Gaussian distribution of relaxation times, thus resulting in a mean hydrodynamic radius r_H, and the width of its Gaussian distribution, σ. The agreement of the particle characterization data with those obtained with our standard setup described below is good.

In case of the charged particles, more complicated relaxation functions were obtained, and the measurements had to be performed with a more complicated setup for combined static and dynamic light scattering consisting of an ALV ISP86 Goniometer and an ALV5000 multitau correlator; the measurements were performed using the 532.8 nm line of a cw frequency doubled, diode pumped Nd-YAG laser (ADLAS 425c) with 300 mW output power. Light scattering experiments for the characterization of the polyelectrolyte structure in highly diluted solutions were carried out in water at 20.0 °C with the mixed bead ion exchange resin inside the cuvette. All solutions were filtered through 0.45 μm Millipore filters.

C. Viscometric measurements

All viscosity measurements were performed in the different solvents at 25.0 °C using an automatic Schott AVS360

Downloaded 28 Aug 2013 to 129.15.14.53. This article is copyrighted as indicated in the abstract. Reuse of AIP content is subject to the terms at: http://jcp.aip.org/about/rights_and_permissions

TABLE I. Polymeranalytical data of all microgels and linear polyelectrolytes used in the examination. R_H denotes the hydrodynamic radius of the parental microlatex in the dispersed state, σ the Gaussian width of the size distribution. The hydrodynamic radii of the purified, but unsulfonated microgels are characterized in four different solvents (THF, DMF, 1,2-dichloroethane, toluene) to estimate the microgel size in the swollen state and to prove its solvent dependence. P_w is the weight average of the number of monomer units in the microgel. For linear polymers, a polydispersity index M_w/M_n is given to characterize polydispersity. Note that the degree of sulfonation is always ~70%, which is adjusted by synthesis.

	R_H^{latex} (nm)	σ	R_H^{THF} (nm)	R_H^{DMF} (nm)	$R_H^{1,2DCE}$ (nm)	$R_H^{toluene}$ (nm)	$[\eta]^{toluene}$ (10^{-3} l/g)	P_w 10^3	Degre of sulfonation
A/3.0/20	7.1	0.25	11.9	11.9	⋯	⋯	⋯	1.18	71%
C/2.0/20	17.8	0.24	25.1	22.8	25.0	24.9	12.0	74.0	69%
C/1.5/20	19.5	0.23	27.3	24.0	27.5	27.8	12.3	103.7	69%
C/0.5/20	26.5	0.24	37.4	35.9	37.6	37.9	11.9	308.9	70%
B/0.1/20	33.7	0.19	52.5	50.6	52.3	52.6	12.4	697.1	68%
B/0.05/20	45.3	0.15	67.8	65.1	67.8	68.0	11.5	1848.5	69%
C/2.0/40	18.4	0.22	37.0	⋯	⋯	⋯	⋯	83.7	72%
C/2.0/80	18.5	0.24	38.2	33.5	⋯	⋯	35.6	85.4	71%
D/1/1	15.5	0.14	⋯	⋯	⋯	⋯	⋯	94.3	⋯
		M_w/M_n							
lin 40	⋯	1.04	⋯	⋯	⋯	⋯	22.3	0.38	72%
lin 100	⋯	1.06	⋯	⋯	⋯	⋯	42.4	0.96	70%
lin 220	⋯	1.05	⋯	⋯	⋯	⋯	73.9	2.11	73%
lin 410	⋯	1.03	⋯	⋯	⋯	⋯	114.5	3.94	75%
lin 698	⋯	1.05	⋯	⋯	⋯	⋯	166.4	6.70	74%

instrument (Ubbelohde viscometers), which allows a reproduction of the flow times with an accuracy of 0.03 s. The solutions were made by dissolving the samples in bidistilled, deionized water; the stock solution was stored over a carefully purified, mixed bead ion exchange resin. The flow times were taken by measuring subsequent dilutions of a stock solution of 10 g/ℓ, and each flow time was reproduced five times. The dilution and the measurements were stopped when the viscosity difference of polyelectrolyte solution and pure water drops below 10%.

IV. RESULTS AND DISCUSSION

A number of different polyelectrolyte microgels was synthesized via polymerization in microemulsion and subsequent polymeranalogous reaction. The molecular properties of these microgels are summarized in Table I. With the different synthetic techniques, we are able to cover the size range of 7 nm$<R<$50 nm; from the viewpoint of crosslinking density, we choose 1/20 (20 monomer units between two crosslinks) as the reference state. In addition, the crosslinking density for just one selected size is varied between a massive colloidal particle (pro forma completely crosslinked) and rather loosely crosslinked particles with 1/80. It must be underlined that all measurements are performed with the polystyrenesulfonic acids, i.e., with the proton as the counterions, since first going experiments showed that the protons produced the highest viscosity effects. This is of experimental importance, since only the polyacids allowed the extension of the measuring range towards the presented small concentrations as well as a suppression of the influence of the autoprotolysis of water. Table I also contains all data of the linear reference standards.

A. Salt dependence of the viscosity of spherical polyelectrolytes

From the viewpoint of discussion, it is best to start with the dependence of the viscosity of charged microgels on the salt concentration, since this experiment allows observation of the slow onset of the electrostatic interaction, where high salt concentrations represent some type of reference state where a charge influence can be neglected. Figure 2 shows the reduced viscosity for sample C/20/40 as a function of polyelectrolyte concentration (g/ℓ) for different salt concen-

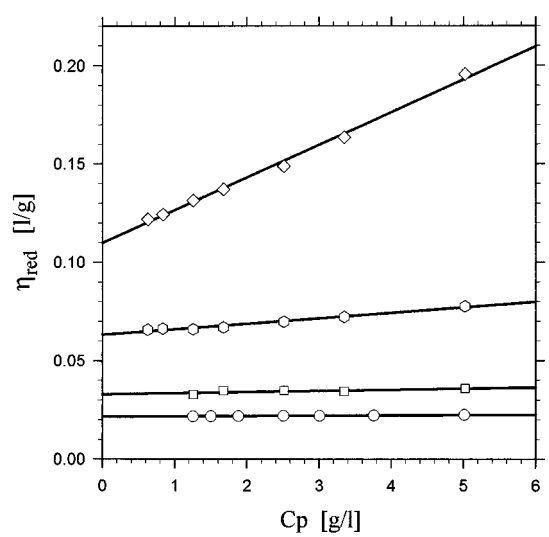

FIG. 2. Viscosity behavior of a spherical polyelectrolyte microgel in presence of different amounts of added low molecular weight salt; (○) $c_S' = 1$ mol/ℓ; (□) $c_S' = 0.1$ mol/ℓ; (○) $c_S' = 0.01$ mol/ℓ; (◇) $c_S' = 0.001$ mol/ℓ. Reducing the salt concentration results in an increase of the reduced viscosity.

Downloaded 28 Aug 2013 to 129.15.14.53. This article is copyrighted as indicated in the abstract. Reuse of AIP content is subject to the terms at: http://jcp.aip.org/about/rights_and_permissions

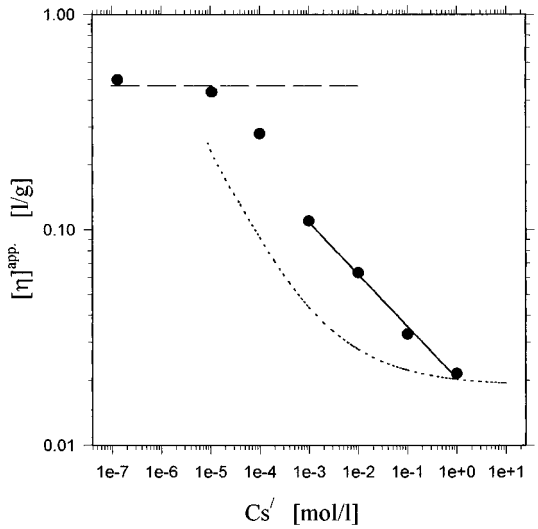

FIG. 3. Dependence of the intrinsic viscosity $[\eta]_0$ (C_s) (reduced viscosity extrapolated to $c_P \rightarrow 0$) on salt concentration c_s. The data above $c_s = 10^{-3}$ mol/L were taken from the linear extrapolation of the viscosity data towards vanishing polymer concentrations. Straight line is a simple scaling analysis of these data. Below $c_s = 10^{-4}$ mol/L, data are obtained by a nonlinear least square fit of the viscosity curves according to Eq. (17). The dotted line sketches the prediction of Eq. (13) with $Z_{\text{eff}} = 19.7$, $R_0 = 37.0$ nm. The dashed line represents the upper limit according to the Bjerrum-shell model and Eq. (15).

TABLE II. Fit parameters used for the quantitative description of theh viscosity data according to Eq. (14). Z_{eff} is the effective charge number per particle, k_H the Huggins-constant. R_0 is the size of the swollen microgels, c_s' is the molar concentration of low molecular weight salt during the measurements. ''s.f.'' denotes the so-called ''salt-free'' case, i.e., deionized water.

	R_0 (nm)	C_s' (mol/L)	Z_{eff}	k_H
C/2.0/40	37.0	s.f.	19.67	0.01
C/2.0/40	37.0	10^{-5}	19.51	0.03
C/2.0/40	37.0	10^{-4}	17.12	0.25
C/2.0/40	37.0	10^{-3}	12.59	1.28
C/2.0/40	37.0	10^{-2}	9.76	0.69
C/2.0/40	37.0	10^{-1}	5.96	0.55
C/2.0/40	37.0	1	1.79	0.37
A/3.0/20	11.9	s.f.	10.78	0
C/2.0/20	25.1	s.f.	13.43	0
C/1.5/20	27.3	s.f.	13.52	0.08
C/0.5/20	37.4	s.f.	13.44	0.82
B/0.1/20	52.5	s.f.	11.61	0
B/.05/20	67.8	s.f.	8.09	0
D/1/1	15.5	s.f.	9.92	0
C/2.0/20	25.1	s.f.	13.43	0
C/1.5/20	27.3	s.f.	13.52	0.08
C/2.0/40	37.0	s.f.	19.68	0.01
C/2.0/80	38.2	s.f.	22.46	0.02

trations ranging from 1 to 10^{-3} mol/ℓ. At the highest salt concentration we observe the lowest viscosity, which is almost independent of polyelectrolyte concentration (the Huggins konstant is $k_H = 0.37$). Upon lowering the salt concentration, the reduced viscosity is steadily increasing.

In the terminology of the Einstein-description, the appearance of some weak electrostatic interactions only increases the effective particle size. The dominance of this type of behavior is clearly restricted to high salt concentrations and low polymer concentrations, i.e., $c_s \gg c_p$. This is related to the behavior of the interaction potential at large r (as compared to κ^{-1}) or the direct correlation function at low q where multiparticle correlations are negligible.

From the intersect with the y-axis, we can extract the intrinsic viscosity, which is clearly a single particle property. The salt dependence of this intersect $[\eta]_0$ is shown in Fig. 3. The high salt data can be approximated by an algebraic function with an exponent of -0.25. The absolute value of $[\eta]_0$ at the highest salt concentration is very similar to the values of this 1:20 microgel in organic solvents like THF, DMF or toluene. Since we do not expect that the increase of the intrinsic viscosity is due to swelling (charge density inside the particles is always rather high, thus suppressing pronounced Coulomb-effects), we attribute this behavior to the build-up of an electrostatic shell where counterions are mutually coupled and act cooperatively also from a hydrodynamic point of view. By all means, this shell is also inpenetrable for other microgels. A reasonable estimate for the size of the shell is given by the balance of thermal energy and electrostatic energy as was introduced above as the Bjerrum shell.

Assuming the measured intrinsic viscosity at $c_s = 1$ mol/L to be equal to $[\eta]_0$, we can use the perturbation approach of Eq. (13) to analyze the increase in effective diameter with decreasing salt concentration. The dotted line indicates this function with $Z_{\text{eff}} = 19.7$ and $R_0 = 37$ nm, the data from Table II. The resulting plateau at high ionic strength as well as the slope of the salt concentration dependence is well predicted, although the complete curve is shifted to lower salt concentrations. The dashed line indicates the limiting value of the intrinsic viscosity according to the Bjerrum sphere model and Eq. (15).

We can alternatively analyze this behavior with Eq. (15) which allows us to extract a salt-dependent effective charge from our data. From the known molecular weight and $[\eta]_0$, we can calculate according to Eq. (2) the viscometric effective radius $R_\eta = (R + r_B)$. Assuming that the geometric radius of the swollen microgel R is always close to the value detected at the high salt limit, we are able to calculate $Z_{\text{eff}}(c_s)$ from r_B. The resulting salt concentration dependence of Z_{eff} is shown in Fig. 4 and will be discussed below in context with the other data included in the figure. Decreasing the salt concentration below $c_s = 10^{-4}$ mol/ℓ distorts the viscosity curves in a way that extrapolation towards zero polymer concentration becomes impossible. Figure 5 shows the complete salt dependence (including the values already presented in Fig. 1) in a double logarithmic scale. At $c_s = 10^{-5}$ mol/ℓ, a maximum occurs in the η_{red}- curve; in the so-called saltfree case, η_{red} is constantly increasing with decreasing concentration, i.e., we observe the polyelectrolyte effect also for spheres.

Using Eqs. (16) and (17), we are able to fit all curves with two parameters, only. The quality of the fit is indicated by the solid lines in Fig. 5, and is—considering the low

Downloaded 28 Aug 2013 to 129.15.14.53. This article is copyrighted as indicated in the abstract. Reuse of AIP content is subject to the terms at: http://jcp.aip.org/about/rights_and_permissions

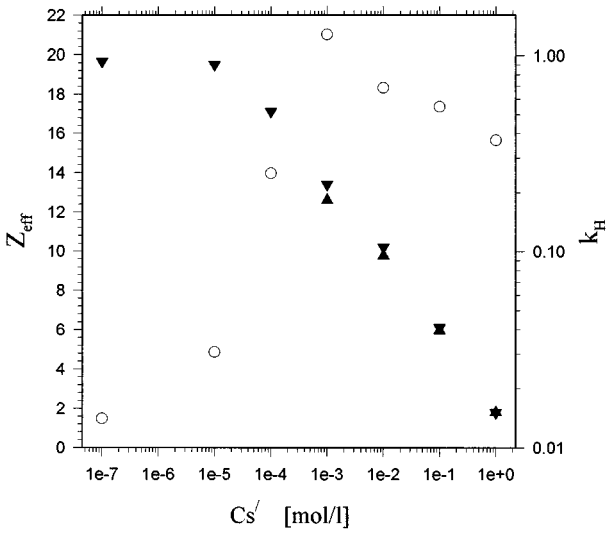

FIG. 4. Salt dependence of the fit parameters Z_{eff} (filled symbols) and k_H (○). The ▲ values are taken from the fit of a Bjerrum shell, whereas the ▼ sign denote Z_{eff} calculated at low salt concentrations by sum approach.

number of free parameters—almost perfect. The resulting fit parameters $Z_{\mathrm{eff}}(c_c')$ and $k_H(c_c')$ are summarized in Table II and were already included in Fig. 4.

Z_{eff} shows a systematic increase with decreasing salt concentration; for low salt concentrations, it levels off for this system to $Z_{\mathrm{eff}} \approx 20$. Very similar number for Z_{eff} were already calculated during the examinations of the viscosity behavior of polyelectrolyte-surfactant complexes in organic solvents.[18] The k_H-value, although fitted without constraints, is for high salt concentrations in the order of the hard sphere value; at $c_s = 10^{-3}$ mol/ℓ where we have the transition behavior, k_H is slightly too large. This might be expected since the neglection of the Green–Kubo crossterms at this critical concentration is a crude oversimplification, and all deviations are righted by k_H. At lower concentrations where the Hess–Klein term is dominating, k_H loses importance, which might be due to the numerical insignificance of this contribution, only. It must be stressed that the presented simple approach holds over three orders of polymer concentration and seven orders of salt concentration, which might be not expected in advance. Moreover, it allows comparison of all data by discussion of one number, Z_{eff} only.

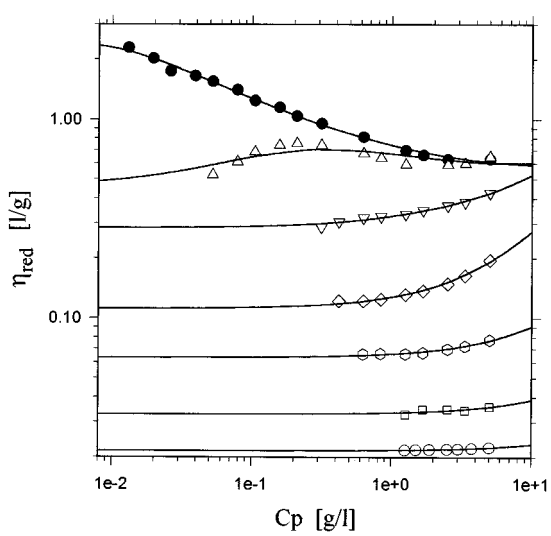

FIG. 5. Dependence of the reduced viscosity of a selected polyelectrolyte sphere over the complete range of salt concentrations in a double-logarithmic presentation; (○) $c_S' = 1$ mol/ℓ; (□) $c_S' = 0.1$ mol/ℓ; (⬡) $c_S' = 0.01$ mol/ℓ; (◇) $c_S' = 10^{-3}$ mol/ℓ; (▽) $c_S' = 10^{-4}$ mol/ℓ; (△) $c_S' = 10^{-5}$ mol/ℓ; (●) ''salt-free'' solutions. The straight lines indicate the two-parameter fit according to Eqs. (17) and (18). The fit function is presented in a broader range than the experimental data to allow estimating of the trends.

At the end of this paragraph, it must be repeated that the reduced viscosity of spherical microgels reacts (even more than linear polyelectrolytes) very sensitive against salt addition; as seen in Fig. 5, a concentration of $c_s = 10^{-5}$ mol/ℓ already drops the reduced viscosity remarkably below the ''pure water''-curve and let a maximum appear. On the one hand, this high salt sensitivity certifies the purity of the samples before salt addition, on the other it also illuminates some of the difficulties of working with these materials in salt-free solutions. All further discussions have to be seen in the light of this sensitivity against ionic purities; although we did our best, salt concentration which might differ from sample to sample and might be in the order of 10^{-6} mol/ℓ cannot be excluded.

B. Size and concentration dependence of the reduced viscosity of spherical polyelectrolytes in salt-free solution

Knowing the behavior of the spherical polyelectrolytes under conditions where they are weakly coupled, we are are able to discuss the behavior under salt-free and strong coupling conditions. Figures 6(a) and 6(b) show the reduced viscosities of the set of microgels with constant crosslinking density 1/20, but varying particle size in saltfree solution where the reduced viscosity is plotted in two different representations on a linear (a) and a logarithmic scale (b) against $\log c_p$. Obviously, the polyelectrolyte effect is characteristic for solutions of all spherical particles. The reduced viscosity of salt free solutions is increasing with decreasing polyelectrolyte concentration. For the smallest particles, the reduced viscosity reaches values as large as 0.66 ℓ/g, a value well above the values of typical uncharged polymers. This magnitude in context with the spherical shape which cannot change with concentration proves that the major component of the polyelectrolyte effect is intermolecular by nature.

Probably due to the restricted concentration range (which is also limited by our conservative decision to stop dilution when the difference to the pure solvent drops below 10%), no maximum of the reduced intrinsic viscosity is observed. As delineated above and described for linear polyelectrolyte,[29–33] we expect a maximum when the ion concentration due to the polymer is of the order of the concentration due to low molecular weight salt. Assuming autoprotolysis of water, only, this is slightly below the experimental range.

Interestingly enough and best seen in the double-

Downloaded 28 Aug 2013 to 129.15.14.53. This article is copyrighted as indicated in the abstract. Reuse of AIP content is subject to the terms at: http://jcp.aip.org/about/rights_and_permissions

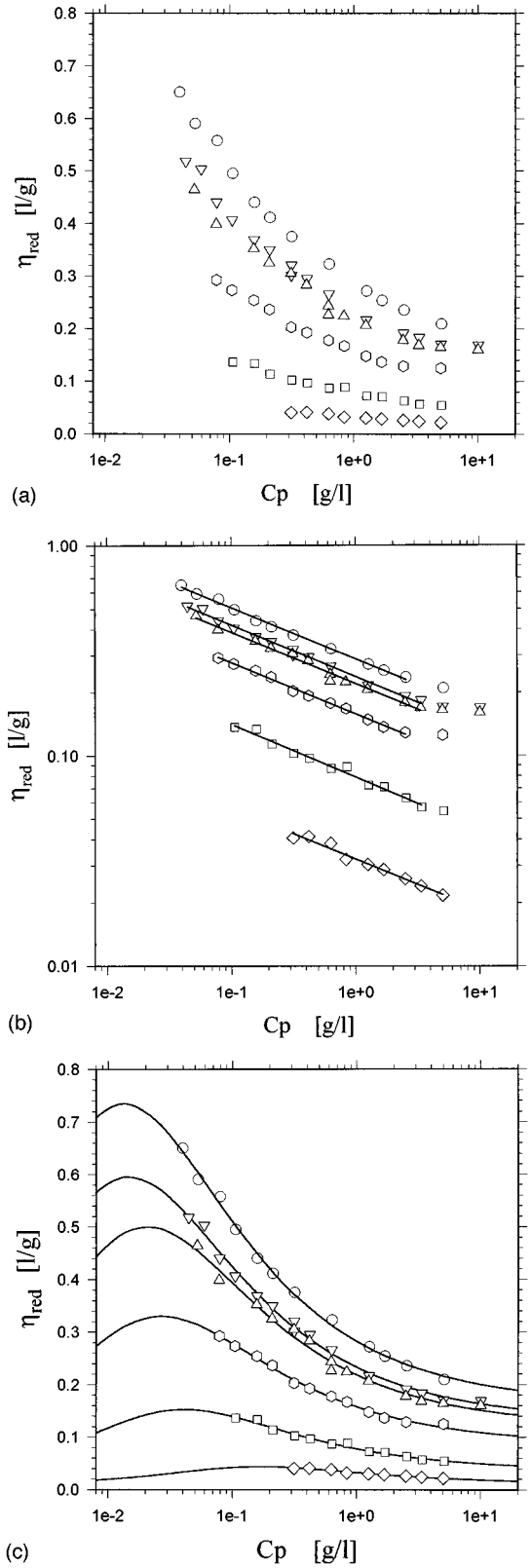

FIG. 6. (a)–(c) Concentration dependence of the intrinsic viscosity of spherical polyelectrolyte microgels with different sizes; (○) 11.9 nm; (▽) 25.1 nm; (△) 27.3 nm; (⬡) 37.4 nm; (□) 52.5 nm; (◇) 67.8 nm. The same data are presented in semilogarithmic (a) as well as in a double-logarithmic plot (b). The straight lines in (b) represent a fit with a scaling law $\eta_{red} \sim c_P^{-0.25}$. (c) shows the fit of the data according to Eqs. (17) and (18) and the fit parameters listed in Table II. Again, the fit function is shown in a much wider range to allow estimating of some trends.

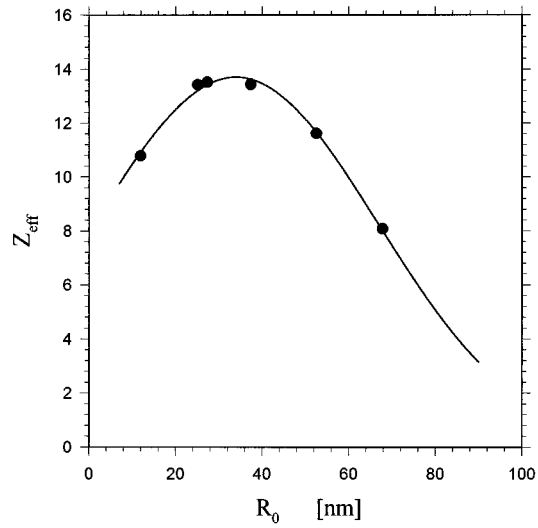

FIG. 7. Dependence of Z_{eff} on the size of the polyelectrolyte microgels, R_0.

logarithmic presentation, the concentration dependencies of the reduced specific viscosity can be described by a scaling law being valid for all particle sizes, given by

$$\eta_{red} \sim c_P^{-0.250 \pm 0.002}. \tag{19}$$

Looking at this dependence, only, and following the discussion given in the theory part, we might explain these data with an electrostatic potential decreasing more rapidly than the screened Coulomb potential, and this interpretation surely cannot be ruled out. A possible expression for the direct correlation function $h(q)$ giving the $-\frac{1}{4}$-dependence was also given above.

On the other hand, the same data can be fitted with high precision by a sum of a hard sphere interaction and a Hess–Klein contribution according to Eqs. (16) and (17). The fit shown in Fig. 6(c) again is almost perfect and is based on Z_{eff} as the only fit parameter. The resulting fit parameters were also summarized in Table II. In all cases, a maximum is predicted which is slightly below the accessible concentration range and which shifts with molecular weight.

Since $[\eta]_0$ is directly related to Z_{eff}, we can also express our fits in terms of $[\eta]_0$. These data are also included in Table II. In all cases, $[\eta]_0$, adds an important contribution to the reduced viscosities which cannot be neglected.

The resulting size dependence of Z_{eff} is shown in Fig. 7. Up to a particle size of $R_0 \approx 40$ nm, Z_{eff} increases as expected. Note that the reduced viscosity has not reached its maximum in the described range of particle sizes (the smallest polyelectrolyte spheres also process the highest viscosities), whereas the maximum is already seen in Z_{eff}. This is due to the influence of the increased particle number density which still counterbalances the slightly decreasing Z_{eff} in a certain size range.

Contrary to all known theoretical descriptions, the fitted Z_{eff}-values are decreasing again when the size of the particles exceeds $R_0 = 40$ nm. No explanation for this behavior can be given, and some theoretical help to understand this experi-

Downloaded 28 Aug 2013 to 129.15.14.53. This article is copyrighted as indicated in the abstract. Reuse of AIP content is subject to the terms at: http://jcp.aip.org/about/rights_and_permissions

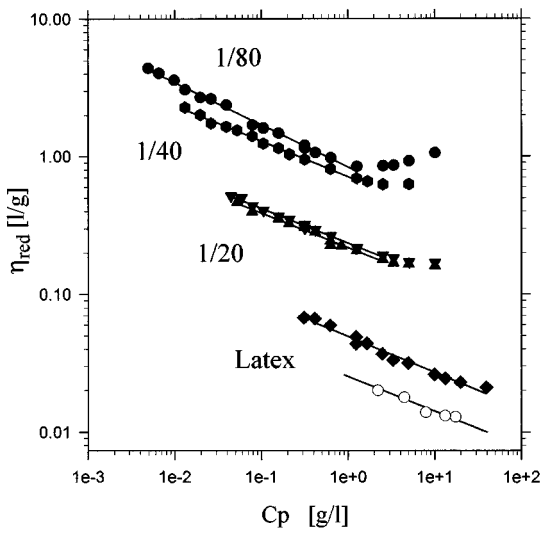

FIG. 8. Dependence of the concentration dependent reduced viscosity on the crosslinking density of the microgels at a fixed molecular weight in a double logarithmic presentation. The viscosity is strongly increasing with decreasing crosslinking density. (●) $p_c=1/80$; (○) $p_c=1/40$; (▼,▲) $p_c=1/20$; (◆) solid latex spheres; (○) sample N100, data of the Ise group.

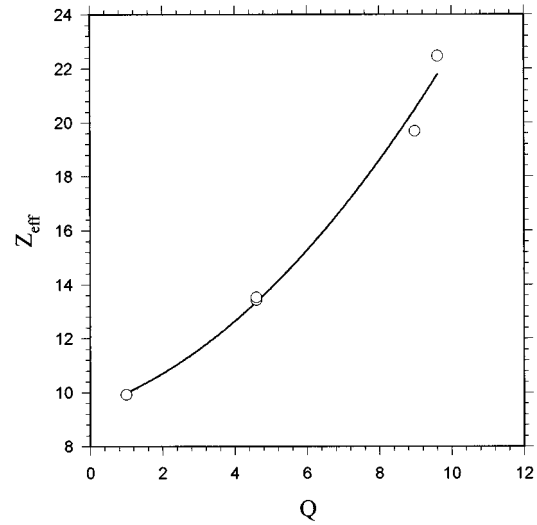

FIG. 9. Dependence of Z_{eff} on the swelling ratio Q of polyelectrolyte microgels at constant molecular weight.

mental finding might be one of the crucial steps towards a better description of charged colloid solutions. It is worth mentioning that our data go well with the rather low reduced viscosities or osmotic moduli described for the larger latex particles with high surface charge density described by the Ise group[12–14] or the Okubo group.[34,35]

Since the description of summing up the Bjerrum sphere- and the Hess–Klein-contribution describes consistently the dependence on salt concentration as well as on polymer concentration, we think that this approach is more appropriate than the simple scaling description involving a nonclassical interaction potential.

C. Dependence of the viscosity on crosslinking density

Another important parameter which is offered by synthesis and which is helpful for learning about the underlying phenomena is the dependence of the reduced viscosity on the crosslinking density at a fixed molecular weight of the microgels. This crosslinking density dependence of the reduced viscosity in salt-free solutions is shown in Fig. 8 in a double logarithmic presentation. The dependence is rather strong. The more looser the particles are crosslinked, the higher are the reduced viscosities. Again, the data of highly charged, solid latex particles and the crosslinking densities $p_c=1/10$, 1/20, and 1/40 exhibit about the same scaling exponent of the concentration dependence; just the most loosely crosslinked microgels (1/80) apparently show a somewhat steeper dependence.

It must be underlined that Fig. 8 also contain data from the Ise group,[12] although on the very bottom of our diagrams (due to the large particles and the related low particle number densities involved), these data essentially show the same behavior like our data.

Again, the fit with the sum approach, the presentation of which is omitted, works almost perfect; the resulting Z_{eff} values were already included in Table II. Even the deviating scaling exponent of the 1/80-sample turns out to be based on a different relative importance of the Hess–Klein term and the additive $[\eta]_0$-term.

Since we have changed by variation of the crosslinking density the swelling ratio Q of the polyelectrolyte microgels at first, it is likely to plot Z_{eff} against Q (Fig. 9). For simplicity, we assume the swelling ratios Q to be independent of added low molecular weight salt (the ionic strength inside the particles is always very high), which enables us to take the hydrodynamic radius of the swollen microgel in 0.1 m NaCl solution. These swelling ratios also compare well with the behavior of uncharged microgels which were discussed in detail in Refs. 36 and 37.

It is seen that the effective charge number is—within experimental error—proportional to the swelling ratio, i.e., the volume of the particle. This is somewhat unexpected, since we are used to talk about surface charges rather than volume charges of colloidal particles, the first going with R^2 as compared to R^3. Again, no arguments for this behavior can be given; it is just that the notation ''effective'' must include a number of complex ion–ion interactions which are rescaled in a still unknown way. Within the framework of this discussion, the Q-dependence is taken as a first experimental observation, only.

From the viewpoint of the viscosity enhancement, it is interesting to note that the 1/80-crosslinked samples already show a very high reduced viscosity. The additional swelling and the related hydrodynamic effects (simple filling of volume) are however negligible as compared to the electrostatic effects, which are indirectly tuned up by a higher effective charge number per microgel particle being proportional to the swelling. This secondary, electrostatic effect is in our opinion mainly responsible for the increase of the reduced viscosity with decreasing crosslinking density, a theme

Downloaded 28 Aug 2013 to 129.15.14.53. This article is copyrighted as indicated in the abstract. Reuse of AIP content is subject to the terms at: http://jcp.aip.org/about/rights_and_permissions

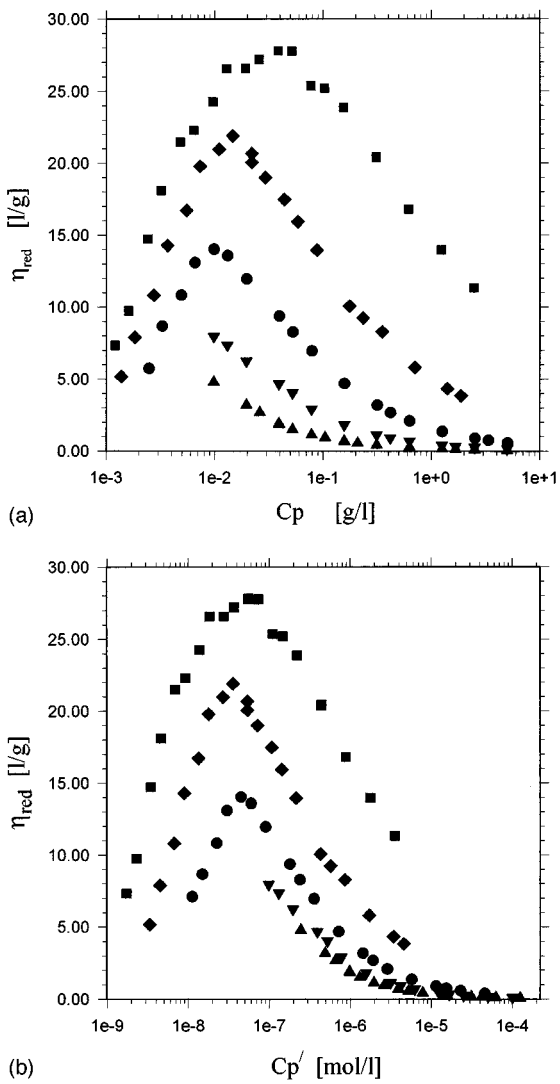

FIG. 10. (a) and (b) Concentration dependence of the reduced viscosity of linear polystyrenesulfonic acids with different molecular weights (▲) 61 kg/mol; (▼) 154 kg/mol; (●) 338 kg/mol; (♦) 630 kg/mol; (■) 1072 kg/mol. The same data are presented in dependence of the weight concentration c_P in g/L (a) as well as in dependence of the molar concentration c'_P in mol/L. Note that the maxima of the reduced viscosities observed for the three higher molecular weights can be superimposed in the molar representation.

which might be important for viscosity behavior of linear polyelectrolytes, too.

D. Comparison with the behavior of linear polyelectrolytes

Since the molecular weight and radii of charged microgels and standard linear polyelectrolytes are not too different, this study offers the unique opportunity to directly compare their viscosity behavior.

Figures 10(a) and 10(b) show a summary of our own data on polystyrenesulfonate in two presentations where the reduced viscosity is plotted vs the polyelectrolyte weight concentration c_p in g/L [Fig. 10(a)] or vs the molar polymer concentration c'_P in mol/L [Fig. 10(b)]. For the three highest molecular weight samples examined, we observe a pronounced maximum of the intrinsic viscosity. Contrary to the earlier experimental findings of Cohen, Priel, and Rabin[29–32] but in good agreement with their later observations,[39] the maximum in our experiments significantly depends on molecular weight and is shifted towards smaller weight concentrations for smaller polyelectrolyte chains. In the molar representation, it becomes obvious that all maxima are located at about the same particle number concentration. Within experimental error, we obtain $c'_P(\max) \approx 4.5 \times 10^{-8}$ mol/ℓ. This positioning is also in good agreement with the later data of Cohen and Priel.[39]

Following diverse model calculations[28] or exact hydrodynamic theories such as the Hess–Klein-approach,[5] the maximum appears close to the point where the molar ion concentration due to the polyelectrolyte and the molar ion concentration due to other species (H^+, OH^-, added low molecular weight salt) are about balanced, e.g., differentiation of the Hess–Klein-equation [Eq. (10)] results in $\Lambda \equiv [Z_{eff} c'_P(\max)/c'_s] = 4$. A Λ- value of 4 as the condition for the maximum was also experimentally confirmed in the work of Cohen *et al.*

Using this condition for the location of the maximum, we might take the ''natural'', minimal ion concentration of water due to autoprotolysis (this is for pure water 2.0×10^{-7} mol/ℓ); note that this is not true for the present case of a strong acid which even reduces the ionic backround), and calculate a $Z_{\mathrm{eff}}\approx10$, independent of molecular weight. However, this number must be regarded as an estimate for a minimal value, only, since the ion balance is highly afflicted with errors due to spurious amount of ionic impurities which can be by a factor larger than the ''natural'' ion concentration. In this context, it is also interesting to discuss the potential of the applied ion exchange resin to bind the last remaining low molecular weight salt pairs, since a thermodynamic equilibrium between polyelectrolyte solution and ion exchange resin for salt binding might be expected.

To avoid rather philosophical discussions about the notation ''pure,'' it is more convincing to elaborate the molecular weight dependence of the peak position and height in presence of controlled low amounts of salt, which was not within the scope of the present paper.

At the present state and concentrating on the qualitative rather than the quantitative aspects of these viscosity curves, we have to live with the fact that the concentration dependent reduced viscosity of all linear polymers with higher molecular weight can be described by a molecular weight independent Z_{eff}, only.

A further discussion of the viscosity curves is better performed on the base of a logarithmic presentation of the same set of data which is shown in Fig. 11. For small linear polyelectrolytes up to 338 K molecular weight, a possible additional $[\eta]_0$-term has no importance since the reduced viscosity curves drop from the maxima to rather low values, each. For the intermediate concentration regime of these polyelectrolytes, the reduced viscosity can be approximated with

Downloaded 28 Aug 2013 to 129.15.14.53. This article is copyrighted as indicated in the abstract. Reuse of AIP content is subject to the terms at: http://jcp.aip.org/about/rights_and_permissions

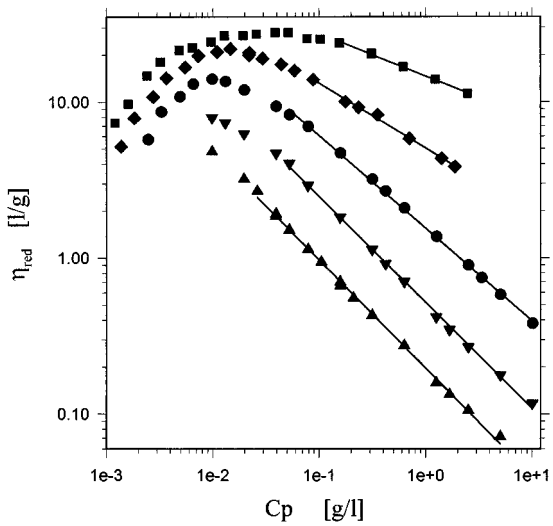

FIG. 11. Concentration dependence of the reduced viscosity of linear polystyrenesulfonic acids [same data and same use of symbols as Figs. 10(a) and 10(b)] in a double-logarithmic plot. The reduced viscosity curves of the linear polyelectrolytes can be fitted in an intermediate concentration regime with scaling laws (straight lines), too, although the exponent depends on molecular weight.

scaling relation, the exponent of which goes from $\alpha=-0.71$ to $\alpha=-0.62$.

It was stated above that the minimal slope which is calculated from reasonable electrostatic potentials is $\alpha=-0.5$, which is the value of a screened Coulomb potential. Therefore, the observed deviations to still smaller values of α reflect the existence of concentration dependent conformational changes. It is worth mentioning that large polyelectrolytes show a less steep behavior, i.e., the conformational changes are more pronounced for the small chains.

For the two highest molecular weights, the concentration regime is too small to get an accurate description with a scaling approach, but values of $\alpha=-0.46$ and $\alpha=-0.27$ might be extracted. The last value for the highest molecular weight sample is already of the order of the α-values of the polyelectrolyte spheres, as the whole curve resembles closely the ones of the polyelectrolyte spheres.

Although a fit with the modified Hess–Klein approach according to Eq. (16) is—in principle—prohibited by the concentration dependent conformational changes, we have applied the sum approach also to the viscosity curves of the linear polyelectrolytes. Since Z_{eff} is fixed by the position of the maximum, all other curve characteristics are mainly adjusted by the hydrodynamic radius r_H, solely. It turned out that all curves can be fitted with this approach, and the resulting hydrodynamic radii are additionally in a reasonable range between 10 nm and 250 nm, depending on molecular weight. On the other hand, the r_H-values can hardly compared with each other, since the parameters react too sensitive towards minor changes of the curve profile and the unknown role of chain expansion.

It is interesting to note that for the larger polymer chains the additive $[\eta]_0$-contribution gains importance again; within our description, this is due to the fact that Z_{eff} does not depend on molecular weight. Consequently, the hydrodynamic contribution of large polyelectrolytes becomes of similar importance as the electrostatic contribution, and the observed change of the viscosity curves is obtained.

From the deviations between theoretical description and experimental data seen for the smaller polyelectrolyte chains, the modified Hess–Klein model even allows us (under assumption of a constant Z_{eff}) to estimate the concentration dependence of coil expansion. Equation (17) tells us that the ratio of the theoretical points to the experimental data is directly proportional to the relative shrinking with respect to the conformation at the viscosity maximum, $r_H(\max)/r_H(c)$. In addition, we can write down the following scaling dependencies:

$$r_H \sim b \cdot N_b^{\nu} \quad \text{and} \quad b \sim c^{-\beta} \Rightarrow r_H(c) \sim c^{-\beta(1-\nu)}. \tag{20}$$

This scaling analysis of polyelectrolyte architecture requires that the number of Kuhn-segments per chain N_b having the length b (including the electrostatic persistence length) is sufficiently large to enable the chosen approximation of the polyelectrolyte conformation as an excluded volume chain with exponent ν.

The experimental analysis of lin 100 for instance gives $r_H(c)=r_H(\max)\cdot c^{-0.2}$; with Eq. (20) and $\nu\approx 0.60$ (self-avoiding walk, see Ref. 40), we obtain for the concentration dependence of the total persistence length $\beta\approx 0.50$. This agrees well with previous measurements supporting the $b\sim\kappa^{-1}$-scaling.

At the end of the discussion we might comment on the observed surprisingly low values of the effective charge, which is in the range of 2–25. This ought to be compared with the number of charged monomers per particle which is of the order of 10^4–10^5 or the number of monomeric charges that can be detected, e.g., by pH electrodes, which is one order of magnitude smaller, i.e., 10^3–10^4, but still three orders of magnitude larger than the values determined by viscosity experiments. At this point we may note that the effective charge in our viscosity measurements characterizes interparticle electrostatic interactions, i.e., the potential energy that one particle experiences in the mean electric field produced by its neighboring particles. Here it is important that local electroneutrality requires most of the counterions to be distributed inside the particle (at $R<R_0$) or near the particle obeying the Poisson–Boltzmann distribution. Conceptually, we may define a distance R' at given salt concentration which is the minimal distance being explored by other colloidal particles and where the major part of the counterion cloud may be located within. The force field of the resulting charge distribution, including dipoles or higher multipoles, either permanent or induced by electrokinetic effects, is approximated with an equivalent point charge with a Debye–Hückel potential, which may indeed be very low.

V. CONCLUSION AND OUTLOOK

It was shown that spherical polyelectrolyte microgels show a strong polyelectrolyte effect in the solution viscosity experiment, thus proving the intermolecular nature of the

Downloaded 28 Aug 2013 to 129.15.14.53. This article is copyrighted as indicated in the abstract. Reuse of AIP content is subject to the terms at: http://jcp.aip.org/about/rights_and_permissions

viscosity enhancement. The observations also support earlier experiments on charged latex particles, which were—due to the much lower particle number density involved—restricted to much lower viscosity enhancements. It was possible to describe the concentration dependence in an intermediate concentration regime with a $\eta_{\mathrm{red}} \sim c_P^{-0.25}$-law, which is not backed by a standard intermolecular potential. On the other hand, we were able to describe the dependence on microgel size as well as the dependence on crosslinking density with a model of spherical particles with an effective charge number Z_{eff}, which act in the frame of a modified Hess–Klein theory. The salt dependence as well as the size dependence of Z_{eff} as the relevant fit parameter was determined. Z_{eff} decreases with increasing salt concentration as expected, but shows an unexpected maximum in its size dependence, the reason for which is still unclear.

It must be underlined that for the examined size range smaller spheres show a larger reduced viscosity than larger spheres, which is exactly opposite to the behavior of linear chain polyelectrolytes. This is due to the reduced particle number of larger spheres at comparable weight concentration which is not sufficiently compensated by a significantly larger Z_{eff} of the larger particles. It is interesting to speculate for which architecture the behavior inverts, i.e., branched polyelectrolytes with a certain branching topology are expected to have even a molecular weight independent reduced viscosity.

Charged microgels with different degrees of crosslinking density and swelling give some indications for the viscosity behavior in dependence of the structural density, the mass of polymer inside a viscometric equivalent sphere. Contrary to all expectations, a behavior where Z_{eff} was roughly proportional to the swelling ratio Q was found, thus resulting in a steep increase of the reduced viscosity for the more open structures. Q enters the formalism only to a minor degree via its hydrodynamic influence, but mainly by increasing the effective charge number.

It was also possible to apply this modified Hess–Klein model (which was developed for charged spheres and successfully applied in this paper for exactly this geometry) to describe the behavior of the solution viscosity of linear polyelectrolytes. It turned out that for different molecular weights, a maximum of the concentration dependent reduced viscosity was found at similar particle number concentrations, i.e., in the standard representation where a weight concentration is used, this maximum shifts proportional to molecular weight.

Within our theoretical model, this is translated in a Z_{eff} which is for linear chains independent of the molecular weight, a finding which is opposite to simple expectations. A molecular weight independent Z_{eff} is however not only backed by the position of the maximum, but also by the quantitative analysis of the shapes of the reduced viscosity curves. The systematic broadening of the maximum of the reduced viscosity with increasing molecular weight as well as the appearance of an additive hydrodynamic viscosity contribution which becomes significant for larger chains can quantitatively be reproduced with the modified Hess–Klein model. In addition, the only other resulting parameter, r_H, turned out to be in a reasonable physical range.

For smaller polyelectrolyte chain with molecular weight below 220 K, a systematic deviation between theoretical description and experimental data became obvious which was attributed to chain extension with decreasing concentration. A rough scaling analysis of the phenomenon revealed that the effect can be described with a persistence length of the chains going with $b \sim c^{-0.5}$, i.e., the same dependence which was recently found with dynamic light scattering.

The whole presented model is reasonable and at least self-consistent, but also sets right the traditional picture of an intramolecular coil-rod transition being responsible for the polyelectrolyte effect, only. Since our modified Hess–Klein approach allows splitting in a (mainly intramolecular) hydrodynamic contribution as well as in a (mainly intermolecular) electrostatic contribution, the relative importance of both components can be filed for all different chain lengths. It turned out that all observed viscosity curves rely on both effects; for smaller polymer chains, the intermolecular, electrostatic effect is certainly the predominant one. For larger chains, the hydrodynamic contribution gives rise to a large viscosity offset and cannot be neglected; although the electrostatic effects still create a typical profile of the viscosity curve, they lose relative importance, which is explained by the molecular weight independent Z_{eff}. Amusingly, this might be a late and partial justification for an hydrodynamic approach.

For future work, it is interesting to extend the ''structural parameter'' used in the present approach and to examine other polyelectrolyte topologies such as branched model systems or rodlike polymers. Obviously, also rods cannot perform any concentration dependent conformational changes, and the resulting concentration–viscosity curve is expected to be similar to the one of the spheres. In the other case, the comparison of those two fixed architectures might enable a statement about the intermolecular potentials involved.

From a practical point of view, such experiments will help optimizing thickeners in terms of the magnitude of thickening as well as their concentration and shear-rate dependence by a quantitative understanding of the counterbalancing roles of molecular topology and charge density and construction of optimized species which make use of their molecular ingredients in the appropriate way.

Another important set of experiments is the electrochemical determination of the concentration of free counterions with appropriate electrodes, in the present case of polysulfonic acids a simple pH-sensor. The determination of the amount of this electrochemically dissociated counterions, its comparison with the value of the ''effective charge number'' seen in the dynamic light scattering experiment, and the relation to Z_{eff} from the viscosity experiment are expected to reveal that the different techniques are sensible towards different subsets of the counterion cloud, which up to now makes a direct relation between the different experiments still very difficult.

In addition, it would be very helpful to extend the presented viscosity measurements towards smaller concentra-

Downloaded 28 Aug 2013 to 129.15.14.53. This article is copyrighted as indicated in the abstract. Reuse of AIP content is subject to the terms at: http://jcp.aip.org/about/rights_and_permissions

tions, at least by one or two orders of magnitude, keeping the high precision of the present data sets. This is clearly out of the instrumental possibilities of a standard Ubbelohde-type capillary viscometer, but might be realized using the instrumental progress in the area of pressure sensors and a capillary geometry with tunable flow. It is expected that this setup enables a more precise determination of the molecular weight dependencies of the position and height of the viscosity maximum, a key feature and a benchmark testing for all current models of polyelectrolyte behavior.

ACKNOWLEDGMENTS

Financial support by the Otto-Röhm-Gedächtnisstiftung, the Deutsche Forschungs-gemeinschaft and the Max Planck Society is gratefully acknowledged. We also want to thank the referee for the real improvement of the theory part.

[1] S. Förster and M. Schmidt, Adv. Polym. Sci. **120**, 53 (1995).
[2] K. S. Schmitz, *Macroions in Solution* (VCH, Weinheim, 1993).
[3] P. J. Flory, *Principles of Polymer Science*, 15th ed. (Cornell University, Cornell, 1992), p. 635.
[4] H. G. Elias, *Makromoleküle* (Hüthig & Wepf, Basel, 1990).
[5] W. Hess and R. Klein, Adv. Phys. **32**, 173 (1983).
[6] Y. Rabin, Phys. Rev. A **35**, 3579 (1987).
[7] R. Borsali, T. A. Vilgis, and M. Benmouna, Macromolecules **25**, 5313 (1992).
[8] S. Förster, M. Schmidt, and M. Antonietti, J. Phys. Chem. **96**, 4008 (1992).
[9] J. Skolnick and M. Fixman, Macromolecules **10**, 944 (1977).
[10] T. Odijk, J. Polym. Sci. Polym. Phys. Ed. **15**, 477 (1977).
[11] M. Schmidt, Macromolecules **24**, 5361 (1991).
[12] J. Yamanaha, H. Matsuoka, H. Kitano, and N. Ise, J. Colloid Interface Sci. **134**, 92 (1990); J. Yamanaha, H. Matsuoka, M. Hasegawa, and N. Ise, J. Am. Chem. Soc. **112**, 587 (1990).
[13] J. Yamanaha, H. Matsuoka, H. Kitano, N. Ise, T. Ymaguchi, S. Saeki, and M. Tsubokawa, Langmuir **7**, 1928 (1991).
[14] J. Yamanaha, H. Araie, H. Matsuoka, H. Kitano, N. Ise, T. Yamaguchi, S. Sachi, and M. Tsubohawa, Macromolecules **24**, 3206, 6156 (1991).
[15] M. Antonietti, W. Bremser, D. Mueschenborn, C. Rosenauer, B. Schupp, and M. Schmidt, Macromolecules **24**, 6636 (1991).
[16] M. Antonietti and T. Nestl, Macromol. Chem. Phys. Rapid Commun. **15**, 111 (1994).
[17] M. Antonietti, R. Basten, and S. Lohmann, Macromol. Chem. Phys. **196**, 441 (1995).
[18] M. Antonietti, S. Förster, M. Zisenis, and J. Conrad, Macromolecules **28**, 2270 (1995).
[19] R. M. Fuoss and J. Strauss, J. Polym. Sci. **3**, 246 (1948).
[20] R. M. Fuoss and J. Strauss, J. Polym. Sci. **3**, 603 (1948).
[21] R. M. Fuoss and J. Strauss, J. Polym. Sci. **4**, 96 (1948).
[22] W. B. Russell, D. A. Saville, and W. R. Schowalter, *Colloidal Dispersions* (Cambridge University, Cambridge, 1989).
[23] H. Vink, Makromol. Chem. **131**, 133 (1970).
[24] A. Briel, Diploma thesis, Marburg, 1993.
[25] M. Antonietti, H. Kaspar, and C. Tauer, Langmuir (submitted).
[26] G. H. Thompson, M. N. Myers, and J. C. Giddings, Anal. Chem. **41**, 1219 (1969).
[27] M. Antonietti, A. Briel, and C. Tank, Acta Polym. **46**, 37 (1995).
[28] C. Schnee, M. Mirke, and M. Schmidt, Polym. Prep. **35**, 52 (1994).
[29] J. Cohen, Z. Priel, and Y. Rabin, J. Polym. Sci. Polym. Lett. **26**, 397 (1988).
[30] J. Cohen, Z. Priel, and Y. Rabin, Polym. Commun. **29**, 235 (1988).
[31] J. Cohen, Z. Priel, and Y. Rabin, J. Chem. Phys. **88**, 7111 (1988).
[32] J. Cohen and Z. Priel, Macromolecules **22**, 2356 (1989).
[33] H. Vink, J. Chem. Soc. Faraday Trans. **83**, 801 (1987).
[34] T. Okubo, J. Chem. Soc. Faraday Trans. **85**, 455 (1989).
[35] T. Okubo, J. Am. Chem. Soc. **112**, 5420 (1990).
[36] M. Antonietti, W. Bremser, and M. Schmidt, Macromolecules **23**, 3796 (1990).
[37] M. Antonietti, in *Rubber Elastic Networks*, edited by J. E. Mark (ICC, Pleasant Hill, 1991), p. 200.
[38] K. S. Schmitz, *An Introduction to Dynamic Light Scattering by Macromolecules* (Academic, Boston, 1990).
[39] J. Cohen and Z. Priel, J. Chem. Phys. **93**, 9062 (1990).
[40] P. G. de Gennes *Scaling Concepts in Polymer Physics* (Cornell University, Ithaca, 1979).

Downloaded 28 Aug 2013 to 129.15.14.53. This article is copyrighted as indicated in the abstract. Reuse of AIP content is subject to the terms at: http://jcp.aip.org/about/rights_and_permissions